Astron. Astrophys. 353, 970–977 (2000)

ASTRONOMY
AND
ASTROPHYSICS

Mass-radius relations for white dwarf stars of different internal compositions

J.A. Panei[⋆], **L.G. Althaus**[⋆⋆], **and O.G. Benvenuto**[⋆⋆⋆]

Facultad de Ciencias Astronómicas y Geofísicas, Paseo del Bosque S/N, (1900) La Plata, Argentina
(panei,althaus,obenvenuto@fcaglp.fcaglp.unlp.edu.ar)

Received 2 March 1999 / Accepted 14 September 1999

Abstract. The purpose of this work is to present accurate and detailed mass-radius relations for white dwarf (WD) models with helium, carbon, oxygen, silicon and iron cores, and with and without a hydrogen envelope, by using a fully updated stellar evolutionary code. We considered masses from 0.15 $\mathrm{M}_{\odot}$ to 0.5 $\mathrm{M}_{\odot}$ for the case of helium core, from 0.45 $\mathrm{M}_{\odot}$ to 1.2 $\mathrm{M}_{\odot}$ for carbon, oxygen and silicon cores, and from 0.45 $\mathrm{M}_{\odot}$ to 1.0 $\mathrm{M}_{\odot}$ for the case of an iron core. In view of the recent measurements made by *Hipparcos* that strongly suggest the existence of WDs with an iron-dominated core, we focus our attention mainly on the finite-temperature, mass-radius relations for WD models with iron interiors. In addition, we explore the effects of gravitational, chemical and thermal diffusion on low mass helium white dwarf models with hydrogen and helium envelopes.

Key words: stars: evolution – stars: fundamental parameters – stars: interiors – stars: white dwarfs

1. Introduction

It is a well known fact that about 90% of stars will end their lives as white dwarf (WD) stars. At present we know different routes that drive stellar objects to such a fate. It is widely accepted, for instance, that low mass WDs with stellar masses $M \lesssim 0.45\ \mathrm{M}_{\odot}$ are composed of helium and that they have had time enough to evolve to such state as a result of binary evolution. For intermediate mass WDs, stellar evolution theory predicts an internal composition dominated by carbon and oxygen. Finally, for the high mass tail of the WD mass distribution, theory predicts interiors made up by neon and magnesium.

Over the years, it has been customary to employ mass-radius relations to confront theoretical predictions on the internal composition of WDs with observational data. This is so because, as it is well known since Hamada & Salpeter (1961) (hereafter HS, see also Shapiro & Teukolsky 1983), zero-temperature configurations are sensitive to the internal composition. One of the effects that allow us to discriminate the WD internal composition for a given stellar mass is related to the dependence of the non-ideal contributions to the equation of state (EOS) of degenerate matter (such as Coulomb interactions and Thomas-Fermi corrections) on the chemical composition. These contributions to the EOS are larger the higher the atomic number Z of the chemical constituent. Another very important effect is that, in the case of heavy elements like iron, nuclei are no longer symmetric ($Z = 26, A = 56$ for iron), yielding a mean molecular weight per electron higher than 2. Accordingly, for a fixed mass value, the WD radius is a decreasing function of Z.

Recently, Provencal et al. (1998) (and other references cited therein) have presented the *Hipparcos* parallaxes for a handful of WDs. These parallaxes have enabled to significantly improve the mass and radius determination of some WDs, thus allowing for a direct confrontation with the predictions of WD theory. In particular, the suspicion that some WDs would fall on the zero-temperature, mass-radius relation consistent with iron cores (see Koester & Chanmugam 1990) has been placed on a firm observational ground by these satellite-based measurements (see Provencal et al. 1998) (however, see below). Indeed, some WDs have much smaller radii than expected if their interior were made of carbon and oxygen, suggesting that, at least, two of the observed WDs have iron-rich cores. Specifically, the present determinations indicate that Procyon B and EG 50 have radii and masses consistent with zero-temperature, iron WDs. Obviously, such results are in strong contradiction with the standard predictions of stellar evolutionary calculations, which allow for an iron-rich interior only in the case of presupernova objects. Although these conclusions are based on the HS zero-temperature, mass-radius relations (note that EG 50 has an effective temperature, $T_{\rm eff}$, of $T_{\rm eff} \approx 21000$ K), it is clear that unless observational determinations are incorrect, the interior of the above-mentioned WDs is much denser than expected before.

Before the above-mentioned determinations, an iron composition has been considered as quite unexpected. In fact, the only attempt of proposing a physical process able to account for the formation of iron WDs is, to our knowledge, that of Isern et al. (1991). In their calculations, Isern et al. find that an explosive ignition of electron-degenerate ONeMg cores may,

Send offprint requests to: J. A. Panei

⋆ Fellow of the Universidad Nacional de La Plata, Argentina

⋆⋆ Fellow of the Consejo Nacional de Investigaciones Científicas y Técnicas (CONICET), Argentina

⋆⋆⋆ Member of the Carrera del Investigador Científico, Comisión de Investigaciones Científicas de la Provincia de Buenos Aires, Argentina

depending critically upon the ignition density and the velocity of the burning front, give rise to the formation of neutron stars, thermonuclear supernovae or iron WDs. It is therefore not surprising that, apart from the study carried out long ago by Savedoff et al. (1969), who did not consider the effects of electrostatic corrections, convection and crystallization in their calculations, very little attention has been paid to the study of the evolution of iron WDs.

We should warn the reader that the existence of WDs with an iron-rich interior is still under debate. In particular, despite recent claims of an iron-rich interior for Procyon B, in the report of this work our referee has told us about a new reanalysis of the observational data which, in a preliminar stage, seems to indicate an interior composition for this object consistent with a carbon one.

Another interesting possibility is that these objects may content some extremely compact core, as proposed by Glendenning et al. (1995a, b). They suggested the existence of stellar objects composed by a strange quark matter (with a density of $\approx 5 \times 10^{14}$ g cm^{-3}) surrounded by an extended, normal matter envelope. These configurations have been called "strange dwarfs". It is presently known that these objects have, for a given mass and chemical composition for the normal matter layers, a much lower radius than a standard WD, and also that they evolve in a very similar way compared to standard WDs (Benvenuto & Althaus 1996a, b). However, at present, it is difficult to account for the formation of a strange quark matter core inside a WD star.

In view of the above considerations, we present in this paper a detailed set of mass-radius relations for WD models with different assumed internal compositions, with the emphasis placed on models with iron-rich composition. Despite the fact that many researchers have addressed the problem of theoretical mass-radius relations for WD of helium (Vennes et al. 1995; Benvenuto & Althaus 1998; Hansen & Phinney 1998 and Driebe et al. 1998), carbon and oxygen (Koester & Schönberner 1986; Wood 1995 amongst others), we judge it to be worthwhile to extend our computations to the case of models with these compositions in the interests of presenting an homogeneous sequence of mass-radius relations. In particular, we shall consider the internal layers as made up by helium (^{4}He), carbon (^{12}C), oxygen (^{16}O), silicon (^{28}Si) and iron (^{56}Fe), surrounded by a helium layer with a thickness of $10^{-2}\ M_*$ (where M_* is the stellar mass). We considered models with an outermost hydrogen layer of $10^{-5}\ M_*$ ($3 \times 10^{-4}\ M_*$ in the case of helium core models) and also models without any hydrogen envelope. In doing so, we shall employ a full stellar evolution code, updated in order to compute the properties of iron-rich, degenerate plasmas properly.

This paper is organized as follows. In Sect. 2, we present the general structure of the computer code that we have employed and the main improvements we have incorporated in it. In Sect. 3, we describe the strategy employed in the computations, and the numerical results. Finally, in Sect. 4, we discuss the main implicances of our results.

2. The computer code

The WD evolutionary code we employed in this study is fully described in Althaus & Benvenuto (1997, 1998), and we refer the reader to those works for a general description. Briefly, the code is based on the technique developed by Kippenhahn et al. (1967) for calculating stellar evolution, and it includes a detailed and updated constitutive physics appropriate to WD stars. In particular, the EOS for the low-density regime is that of Saumon et al. (1995) for hydrogen and helium plasmas, whilst the treatment for the completely ionized, high-density regime includes ionic contributions, coulomb interactions, partially degenerate electrons, electron exchange and Thomas-Fermi contributions at finite temperature. Radiative opacitites for the high-temperature regime ($T \geq 6000$ K) with metallicity $Z = 0$ are those of OPAL (Iglesias & Rogers 1993), whilst for lower temperatures we use the Alexander & Ferguson (1994) molecular opacities.

High-density conductive opacities and the various mechanisms of neutrinos emission for different chemical composition (^{4}He, ^{12}C, ^{16}O, ^{20}Ne, ^{24}Mg, ^{28}Si, ^{32}S, ^{40}Ca and ^{56}Fe) are taken from the works of Itoh and collaborators (see Althaus & Benvenuto 1997 for details). In addition to this, we include conductive opacities and Bremsstrahlung neutrinos for the crystalline lattice phase following Itoh et al. (1984a) and Itoh et al. (1984b; see also erratum Itoh et al. 1987), respectively. The latter becomes relevant for WD models with iron core since these models begin to develop a crystalline core at high luminosities (up to two orders of magnitude higher than the luminosity at which a carbon-oxygen WD of the same mass begins to crystallize). With respect to the energy transport by convection, for the sake of simplicity, we adopt the mixing length prescription usually employed in most WD studies. This choice has no effect on the radius of the models. Finally, we consider the release of latent heat during crystallization in the same way as in Benvenuto & Althaus (1997).

As in our previous works on WDs, we started the computations from initial models at a far higher luminosity than that corresponding to the most luminous models considered as meaningful in this paper. The procedure we follow to construct the initial models of different stellar masses and internal chemical composition is based on an artificial evolutionary procedure described in our previous papers cited above. In particular, to produce luminous enough initial models, we considered an artificial energy release. After such "heating", models experience a transitory relaxation to the desired WD structure. Obviously, the initial evolution of our WD models is affected by this procedure but, for the range of luminosity and $T_{\rm eff}$ values considered in this paper this is no longer relevant (see below) and our mass-radius relations are completely meaningful.

3. Numerical results

In order to compute accurate mass-radius relations, we evolved WD models with masses ranging from 0.15 $\mathrm{M}_\odot$ to 0.5 $\mathrm{M}_\odot$ at intervals of 5% for helium core WDs; from 0.45 $\mathrm{M}_\odot$ to 1.2 $\mathrm{M}_\odot$ at intervals of 0.01 $\mathrm{M}_\odot$ for carbon, oxygen and silicon cores;

and finally from 0.45 $M_\odot$ to 1.0 $M_\odot$ for the case of an iron core at intervals of 0.01 $M_\odot$. The evolutionary sequences were computed down to $\log L/L_\odot$= -5. Mass-radius relations for interior compositions of ^{12}C, ^{16}O, ^{28}Si and ^{56}Fe are presented for $T_{\rm eff}$ values ranging from $T_{\rm eff}$= 5000K to 55000 K with steps of 10000 K and from 70000 to 145000 K with steps of 15000 K. For the case of helium WD models we considered $T_{\rm eff}$ values from $T_{\rm eff}$= 4000 K to 20000 K with steps of 4000 K. To explore the sensitivity of our results to a hydrogen envelope, we considered two values: $M_{\rm H}/M_* = 10^{-5}$ (3×10^{-4} M_* in the case of He core models) and $M_{\rm H}/M_* = 0$. For the sake of comparison, for each of the considered core compositions we have also computed the zero-temperature HS models.

It is worth noting that all the models included in the present work have densities below the neutronization threshold for each chemical composition (1.37×10^{11} g cm^{-3} for helium, 3.90×10^{10} g cm^{-3} for carbon, 1.90×10^{10} g cm^{-3} for oxygen, 1.97×10^{9} g cm^{-3} for silicon, and 1.14×10^{9} g cm^{-3} for iron). Such densities represent the end of the WD sequences because electron capture softens the EOS and the stellar structure becomes unstable against gravitational collapse (see Shapiro & Teukolsky 1983 for further details).

In recent years, both observational (Marsh 1995; Moran et al. 1997; Landsman et al. 1997; Edmonds et al. 1999 amongst others) and theoretical (Althaus & Benvenuto 1997, Benvenuto & Althaus 1998, Hansen & Phinney 1998, Driebe et al. 1998) efforts have been devoted to the study of helium WDs. It is now accepted that these objects would be the result of the evolution of certain binary systems, in which mass transfer episodes would lead to the formation of helium degenerates within a Hubble time (see, e.g., Iben & Tutukov 1986; Alberts et al 1996; Ergma & Sarna 1996). Connected with the age determination for millisecond pulsars from WD cooling is the existence or not of hydrogen flashes in helium WDs. In particular, detailed calculations predict that hydrogen flashes do not occur on WDs of mass less than 0.2 $M_\odot$ (see also Driebe et al. 1998), but instead such low-mass helium degenerates experience long-lasting phases of hydrogen burning (but see Sarna et al. 1998).

With regard to the main topic of the present work, it is worth mentioning that Vennes et al. (1995) presented a set of static mass-radius relations for hot WDs However, the authors considered a linear relation between the internal luminosity and the mass, thus avoiding the computation of evolutionary sequences. This approximation is equivalent to neglecting neutrino emission, which is not a good assumption for their hottest models.

In a recent paper, Driebe et al. (1998) have computed the evolution of low mass stars from the main sequence up to the stage of helium WD. In that work the binary evolution has been mimicked by applying, at appropriate positions, large mass loss rates from a single star. More importantly, diffusion was neglected throughout the entire evolution. In this connection, gravitationally induced diffusion is expected to lead to noticeable changes in the surface gravity of their helium WD models, the envelope of which at the end of mass loss phase is a mixture of helium and hydrogen. Indeed, during their evolution, WDs should modify the outer layers chemical composition making essentially the bulk of the hydrogen float to the surface and the helium sink out of surface layers. In this way, this effect causes the outer layers composition to approach to pure composition layers, the case we assumed in the present paper. Preliminary results to be presented below indicate this to be the actual case, as we suggested previously (Benvenuto & Althaus 1999).

To address the problem of diffusion in helium WDs, we have developed a code which solves the equations describing gravitational settling and chemical and thermal diffusion. Here, we present some details of our code, deferring a thorough description to a further publication. In broad outline, we have solved the diffusion and heat flow equations presented by Burgers (1969) for the case of a multicomponent medium appropriate for the case we are studying here (see also Muchmore 1984 for an application of the set of Burgers's equations to the study of diffusion in WDs). The resistence coefficients are from Paquette et al. (1986). To solve the continuity equation we have generalized the semi-implicit finite difference method presented by Iben & McDonald (1985) to include the effects of thermal diffusion. We have followed the evolution of the isotopes ^{1}H, ^{3}He, ^{4}He, ^{12}C and ^{16}O. The diffusion code has been coupled to our evolutionary code to follow the chemical evolution of our models self-consistently.

Let us first compare our models with those of Driebe et al. (1998) in the case when diffusion is neglected. In Fig. 1 we show the surface gravity in terms of $T_{\rm eff}$ for 0.195 and 0.3 $M_\odot$ helium WD models. In order to make a direct comparison with Driebe et al.'s predictions, we have adopted for these models the same envelope mass and hydrogen surface abundance as quoted by these authors. The initial models were generated in the same fashion as described previously. Despite the assertions by Driebe et al., note that our gravity values after the relaxation phase of our models are very similar to those predicted by these authors. We should remark that their "contracting models" are very different from our initial ones. In fact, they start with a homogeneous main sequence model in which nuclear energy release has been suppressed. Then, it is not surprising that they get contracting models with gravities comparable to those obtained with evolutionary models only when they are very cool (at $T_{\rm eff} \approx$ 3000K for a 0.2 $M_\odot$ model). On the contrary, in our previous works on helium WDs with hydrogen envelopes, we generated our initial models from a cool helium WD model, adding to it an artificial energy release up to the moment in which the model is very luminous. Then, we switch it off smoothly, getting a model very close to the cooling branch. Thus, notwithstanding Driebe et al. comments, our artificial procedure gives rise to mass-radius relations in good agreement with those found with a fully evolutionary computation of the stages previous to the WD phase. A further comparison performed with low-mass helium WD models calculated by Hansen & Phinney (1998) with thick hydrogen envelopes reinforces our assertion. However, for more massive models some divergences appear between our results and those of Hansen & Phinney. Such differences are the result of the fact that Hansen & Phinney massive models do not converge to the HS predictions for zero temperature configurations, a limit to which our models tend.

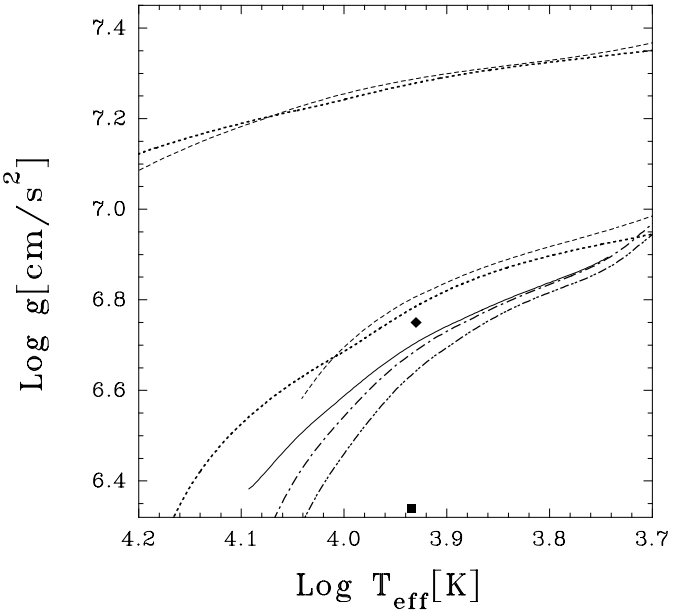

Fig. 1. Surface gravity versus $T_{\rm eff}$ for 0.3 (upper curves) and 0.195 (lower curves) $M_\odot$ helium WD models. Dotted lines correspond to models calculated by Driebe et al. (1998). Dashed lines represent our models with an envelope mass of $1.2 \times 10^{-3} M_\odot$ (with a hydrogen content by mass of $X_{\rm H}$= 0.538) and $6 \times 10^{-4} M_\odot$ (with $X_{\rm H}$= 0.7) for the 0.195 and 0.3 $M_\odot$ models, respectively. Solid line corresponds to the case when diffusion is included in our 0.195 $M_\odot$ model with an envelope of $1.2 \times 10^{-3} M_\odot$ and an initial $X_{\rm H}$= 0.538, while dot-dashed lines and dot-dot-dashed lines are for our 0.195 $M_\odot$ models with pure hydrogen envelopes with mass of 6×10^{-4} and 1.2×10^{-3} $M_\odot$, respectively. The location of the WD companion to the millisecond pulsar PSR J1012 + 5307 according to van Kerkwijk et al. (1996) and Callanan et al. (1998) determinations (upper and lower square, respectively) are also indicated.

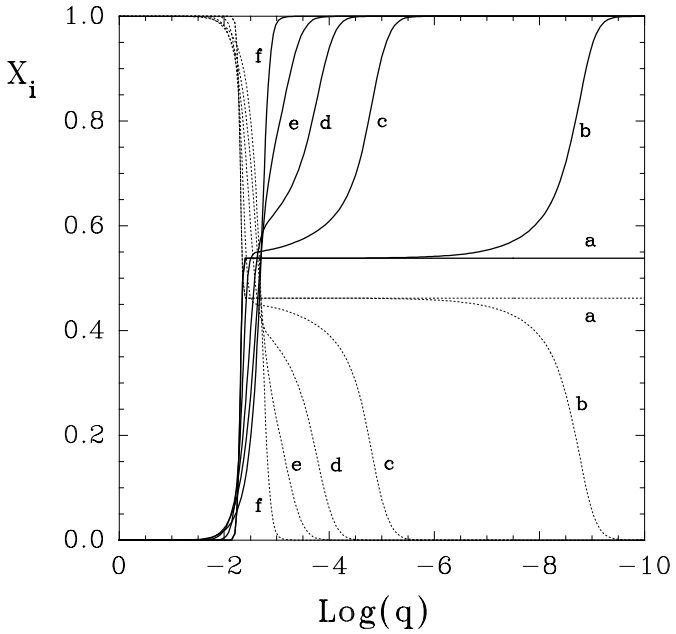

Fig. 2. Evolution of the hydrogen (solid lines) and helium (dotted lines) profiles as a function of the outer mass fraction q for the 0.195 $M_\odot$ helium WD model. Starting out from a model with an initially homogenous envelope with $X_{\rm H}$= 0.538 (curves a), following models (b, c, d, e and f) correspond to evolutionary stages characterized by log $T_{\rm eff}$= 4.096, 4.063, 4.0, 3.932 and 3.762.

Now, let us consider what happens when diffusion is considered. To this end, we have computed the evolution of a 0.195 $M_\odot$ helium WD model with an envelope characterized by a mass fraction $M_{\rm env}/M_* = 6 \times 10^{-3}$ and an abundance by mass of hydrogen ($X_{\rm H}$) of 0.538, as quoted in Driebe et al. (1998). We begin by examining Fig. 2 in which we show the evolution of the hydrogen and helium profiles as a function of the internal mass fraction for various selected values of $T_{\rm eff}$. Even in this case of low surface gravity, diffusion proceeds in a very short timescale, giving rise to pure hydrogen outermost layers. If we start out the computations at $T_{\rm eff} \approx$ 4.1, we find that at the $T_{\rm eff}$ value corresponding to the WD companion to PSR J1012 + 5307, our model is characterized by a pure hydrogen envelope of $M_{\rm env}/M_* \approx 4 \times 10^{-4}$ (curve e). Needless to say, this will affect the surface gravity as compared with the case when diffusion is neglected. Thus, in order to accurately estimate the mass of that WD we do need to account for the diffusion process. This expectation is borne out by Fig. 1, in which we have included the results corresponding to the situation when diffusion is included (solid line) and to the case of the model with assumed pure hydrogen outer layers (dot dashed lines) throughout its entire evolution (i.e. the conditions we would have it were diffusion instantaneous). In both situations we assumed that the total initial amount of hydrogen is the same. The differences in the value of the surface gravity compared with the case of no diffusion are noticeable. Finally, note that the track asymptotically merges the corresponding to complete separation of hydrogen and helium, the structures we assumed in our previous works. These results clearly justifies the assumptions we made in our referred papers. We should also note that in the case of a somewhat thicker hydrogen envelope, hydrogen burning increases significantly, thus making the evolution considerably slower. Thus, in the plane surface gravity versus $T_{\rm eff}$, the asymptotic conditions of total separation of hydrogen and helium would be reached far earlier in the evolution. Thus, diffusion is a fundamental ingredient if we want a solid surface gravity versus $T_{\rm eff}$ relation.

In Fig. 3, we show the mass-radius relation for helium core models. We considered models with masses up to 0.5 $M_\odot$ because higher mass objects should be able to ignite helium during previous evolutionary stages and should not end their lives as helium WDs. As it is well known, models have a larger radius the higher the $T_{\rm eff}$. It is also clearly noticeable the effect on the stellar radius induced by the presence of an outer hydrogen envelope. These effects are particularly important for low mass models. Let us consider the case of a 0.3 $M_\odot$ helium WD model. In the case of no hydrogen envelope, at the highest $T_{\rm eff}$ considered here, the object has a radius ≈50% larger than that corresponding to the HS model. If we include the hydrogen envelope, the radius is ≈80% larger than the HS one (let us remind the reader that in this case we have included a hydrogen layer

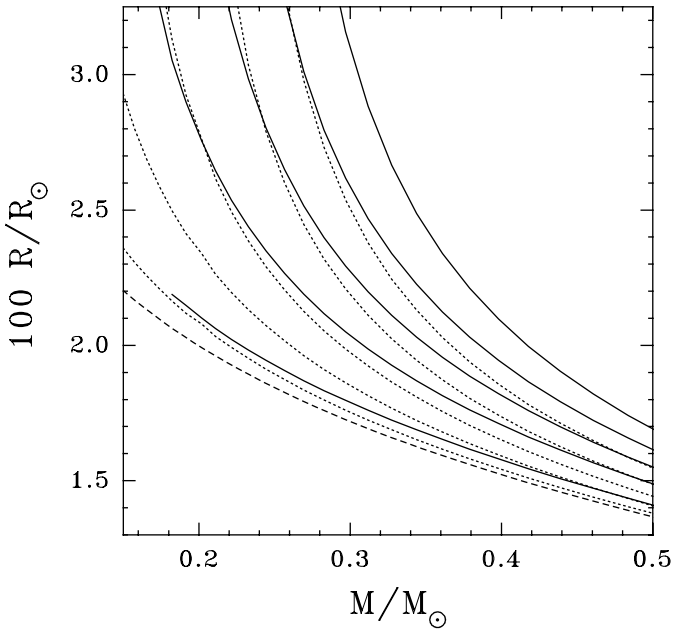

Fig. 3. The mass-radius relation for WD stars with a helium core. Solid and short dashed lines correspond to the cases of objects with an outermost pure hydrogen layer of $3 \times 10^{-4}\ M_*$ and to models without hydrogen layer, respectively. Medium dashed line represent the mass-radius relation for HS homogeneous helium models. Finite temperature models are ordered from bottom to top with increasing $T_{\rm eff}$ correspnding to (in 10^3 K) of 4, 8, 12, 16, and 20.

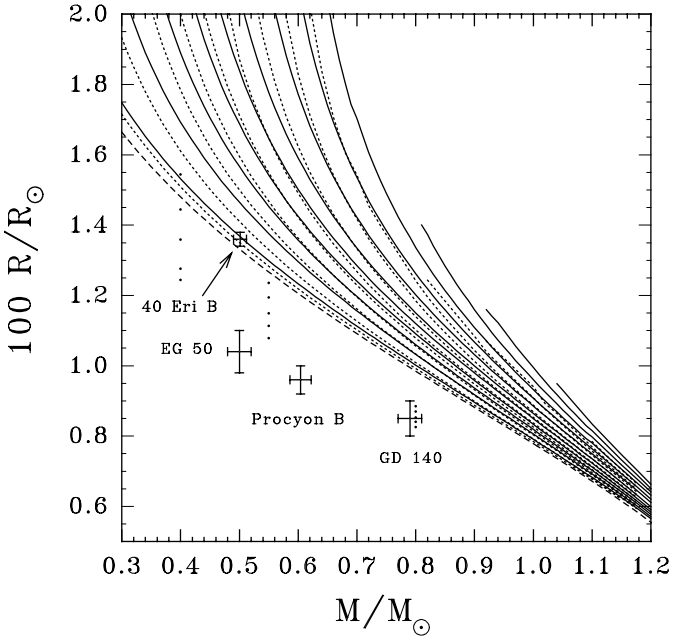

Fig. 4a. The mass-radius relation for WD stars with a carbon core surrounded by a helium layer with a thickness of $10^{-2}\ M_*$. Solid and short dashed lines have the same meaning as in Fig. 3 but for case of the hydrogen envelope we assumed a mass of $10^{-5}\ M_*$. Medium dashed line corresponds to the mass-radius relationship for homogeneous HS carbon models. We have included in this figure the values corresponding to $T_{\rm eff}$ (in 10^3 K) of 5, 15, 25, 35, 45, 55, 70, 85, 100, 115, 130 and 145. We have also included the data for strange dwarf models with $T_{\rm eff}$ (in 10^3 K) of 10, 20, 30, 40 and 50. Notice that they are much more compact than standard WD models with the same composition and mass. In the interests of completeness, we have extended the computations to a mass value of 0.3 $\mathrm{M}_\odot$.

30 times more massive than in the case of the other core compositions). Notice that for $T_{\rm eff} \to 0$, the radius of the objects tends to the HS values, as expected.

In Figs. 4 to 6 we show the results for carbon, oxygen and silicon interiors respectively. Although the effects due to finite temperature and the presence of an outer hydrogen envelope are also noticeable, these are not so large as in the case of the low mass helium WD models shown in the previous figure. For example, for 1.2 $\mathrm{M}_\odot$ models, both effects are able to inflate the star only up to $\lesssim 19\%$. This is expected because as mass increases, internal density (and electron chemical potential μ_e) also increases. Thus, as thermal effects enter the EOS of the degenerate gas as a correction $\propto (T/\mu_e)^2$, EOS gets closer to the zero temperature behaviour, i.e. to the HS structure. As the thickness of the hydrogen layer is $\propto g^{-1}$ (g is the surface gravity) it also tends to zero for very massive models. Note that carbon, oxygen and silicon have a mean molecular weight per electron very near 2 ($\mu_e = 2.001299$, 2.000000, 1.999364, and 1.998352 for helium, carbon, oxygen and silicon respectively), thus, the differences in radii for a given stellar mass are almost entirely due to the non-ideal, corrective terms of the EOS. Because of this, the differences in radii are small, of the order of few percents. Also, in each figure we included the corresponding HS sequence. Notice that, for a given mass value, HS models have smaller radii and that there exist some minute differences even for the lowest $T_{\rm eff}$ models. This is due simply to the presence of a helium (and hydrogen) layer (if present), the effect of which

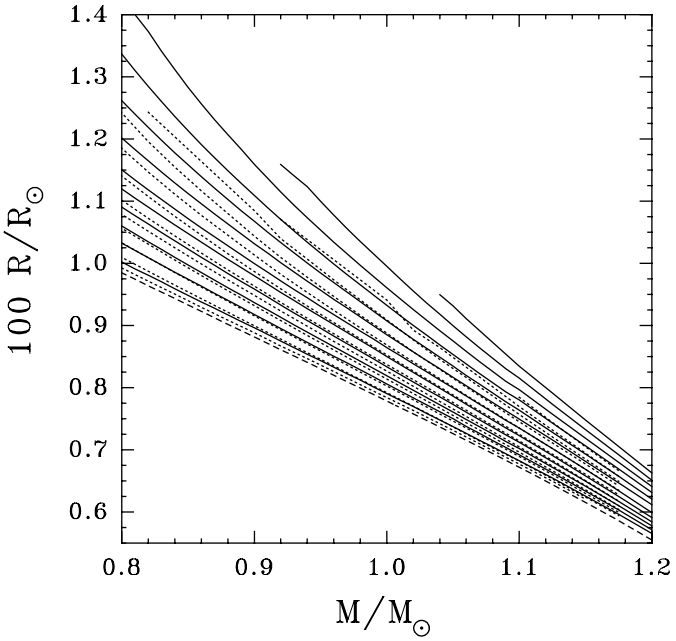

Fig. 4b. Same as Fig. 4a, but for the massive carbon core models.

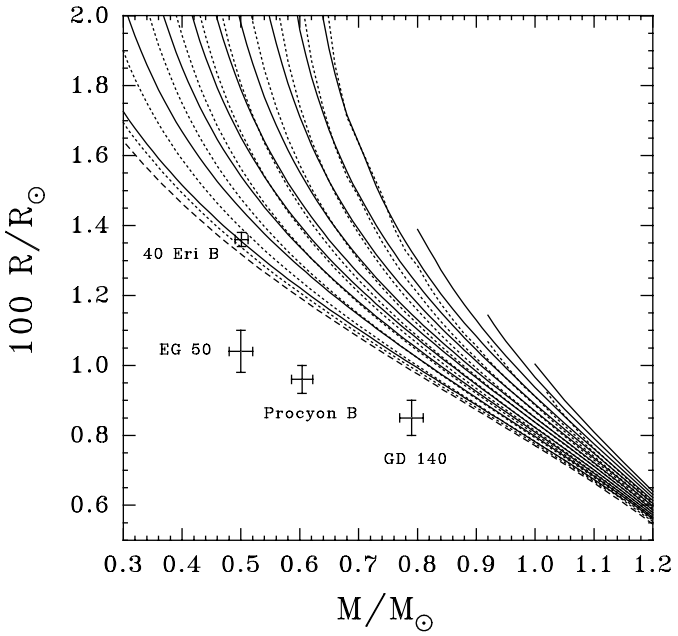

Fig. 5. Same as Fig. 4a, but for an oxygen core.

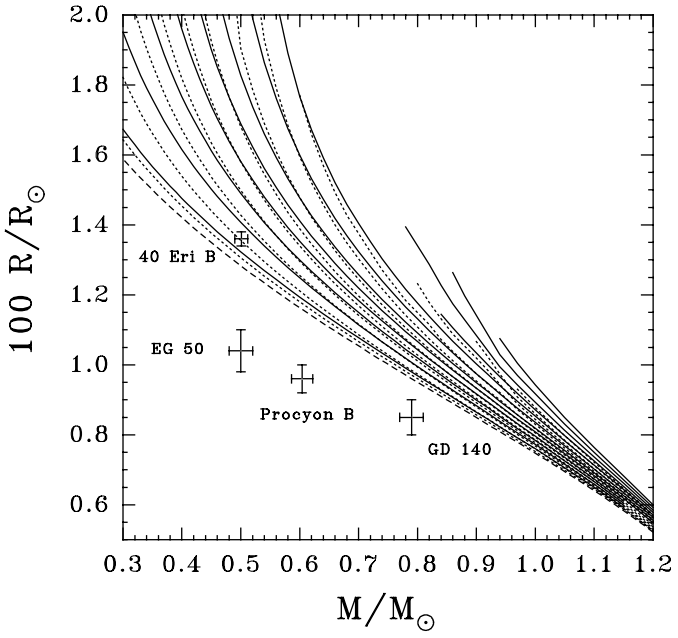

Fig. 6. Same as Fig. 4a, but for a silicon core.

on the model radius was not considered in our computation of the HS sequences.

In Fig. 4a we also included the radii corresponding to strange dwarfs of 0.4, 0.55 and 0.8 $\mathrm{M}_\odot$ models for $T_{\rm eff}$ from $T_{\rm eff}$ = 10000 K to 50000 with steps of 10000 K. These objects were computed assuming a carbon-oxygen composition for the normal matter envelope, but despite the precise chemical profile, it is clear that they have much smaller radii than WD models of the same mass.

In Fig. 7, we show the mass-radius sequences corresponding to iron. These are noticeably different from the previously shown, due mainly to the higher mean molecular weight per

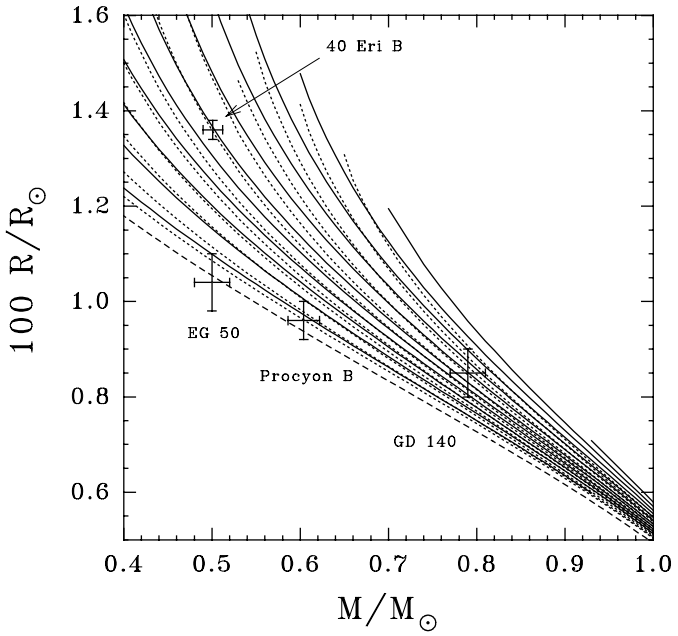

Fig. 7. Same as Fig. 4a, but for an iron core. We have also included the data corresponding to 40 Eri B, EG 50, Procyon B and GD 140 taken from Provencal et al. (1998). Note the change in the vertical scale compared to the previous figures. For further discussion, see text.

electron ($\mu_e = 2.151344$) and also to the much higher atomic number ($Z = 26$) that indicates a much strongly interacting, degenerate gas compared to the case of a standard composition.

In the case of an iron core, for a fixed mass value, the mean density is almost twice the corresponding to carbon and oxygen cores. Thus, it is not surprising that, for the range of $T_{\rm eff}$'s considered here, thermal effects are less important than in the standard case. For example, for the 0.45 $\mathrm{M}_\odot$ iron model at $T_{\rm eff}\approx$ 25000K, thermal effects inflate its radius only by $\approx 17\%$. For the iron core case, we have only considered models up to a mass value of 1.0 $\mathrm{M}_\odot$. Higher mass objects are very near the mass limit for such composition (i.e. the central density becomes very near the neutronization threshold, see also Koester & Chanmugam 1990) and would have internal densities so high that our description of the EOS would not be accurate enough for our purposes. The evolutionary sequences corresponding to an iron core composition are the most detailed and accurate computed to date, and a thorough discussion of them will be deferred to a separate publication.

Finally, in Fig. 8 we compare the results of our calculations for carbon WD models with a hydrogen envelope against the computations performed by Wood (1995). As we mentioned, the mass-radius relation have been the subject of many authors, amongst others, Koester 1978, Iben & Tutukov (1984), Mazzitelli & D'Antona (1986), Wood (1995). Here, we shall compare with Wood's models since they have been thorougly employed by the WD community. Note that the general trend of our results and those of Wood is very similar. As Wood considered more massive hydrogen envelopes ($M_{\rm H}/M_* = 10^{-4}$) than we did, we have recomputed models with 0.6, 0.7 and 0.8 $\mathrm{M}_\odot$ and with

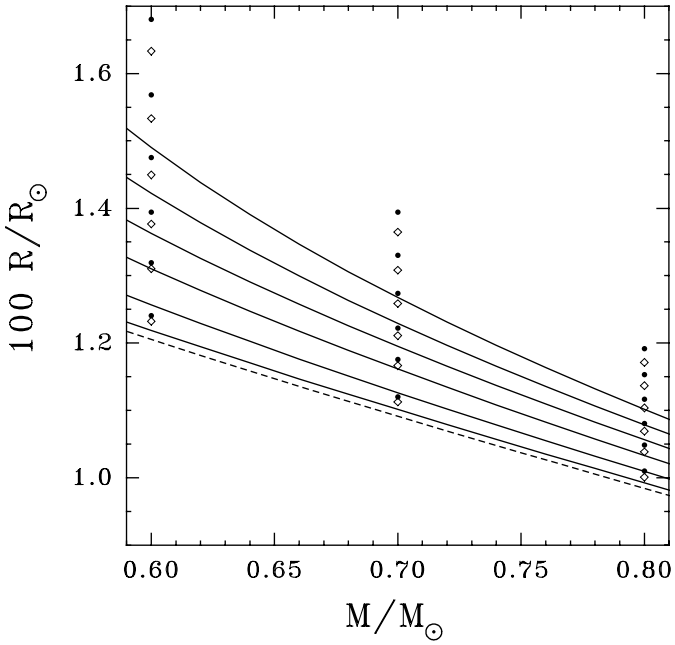

Fig. 8. A comparison of our results with those of Wood (1995). Solid lines indicate the previously presented results for carbon core models including an outer hydrogen envelope, solid dots indicate the results of Wood. As Wood considers more massive hydrogen layers ($M_{\rm H}/M_* = 10^{-4}$) than the one employed in most of this work, we have computed also models with the same hydrogen mass envelope. The results corresponding to these models are denoted with open diamonds.

that hydrogen mass. We find that, for the same value of $M_{\rm H}/M_*$, Wood models have radii a bit larger than ours (of course, for the case of $M_{\rm H}/M_* = 10^{-5}$ the differences are much larger). Note that as models evolve, such differences become smaller.

4. Discussion and conclusions

In this work, we have computed accurate and detailed mass-radius relations for white dwarf (WD) stars with different core chemical compositions. In particular we have considered interiors made up by helium, carbon, oxygen, silicon and iron surrounded by a helium layer containing 1% of the stellar mass. With regard to the presence of a hydrogen envelope, we have considered two extreme values: $M_{\rm H}/M_* = 10^{-5}$ ($M_{\rm H}/M_* = 3 \times 10^{-4}$ for helium core models) and $M_{\rm H}/M_* = 0$. The first three interior compositions are standard (according to stellar evolution theory), whereas iron-rich interiors has recently been suggested on the basis of new parallax determinations for some objects (Provencal et al. 1998).

For computing each sequence we employed a full stellar evolutionary code which incorporates most of the currently physical processes considered relevant to the physics of WDs. We computed a set of evolutionary sequences for each considered core composition by employing a small step in the stellar mass. We believe that these calculations may be valuable for the interpretation of future observations of this type of WDs.

We have also investigated the effect of gravitational settling and chemical and thermal diffusion on low-mass helium WDs with envelopes made up of a mixture of hydrogen and helium. To this end, we included in our evolutionary code a set of routines which solve the diffusion and heat flow equations for a multicomponent medium. For the case analysed in this paper, we found that diffusion gives rise to appreciable changes in the theoretical mass-radius relation, as compared with the case when diffusion is not considered (Driebe et al. 1998).

In Figs. 4-7 we included the data for 40 Eri B ($T_{\rm eff}$=16700 K), EG 50 ($T_{\rm eff}$=21000 K), Procyon B ($T_{\rm eff}$=8688 K) and GD 140 ($T_{\rm eff}$=21700 K) taken from Provencal et al. (1998). In the case of 40 Eri B for instance, the observed mass, radius and $T_{\rm eff}$ are consistent with models having a carbon, oxygen and silicon interior and thin hydrogen envelopes. It is worth noting that the observed determinations are also consistent with iron core models with hydrogen envelope composition but for models with ≈ 55000 K (models without hydrogen envelope would need to be even hotter). Since this temperature is far larger than the observed one we should discard an iron core for this object.

On the contrary, for the cases of the other considered objects, they fall clearly below the standard composition sequences, indicating a denser interior. If we assume GD 140 and Procyon B to have an iron core, we find that they fall on a sequence of a $T_{\rm eff}$ compatible with the observed value. Nevertheless, the EG 50 mean radius is smaller than predicted for an iron core object for the observed $T_{\rm eff}$. Thus, on the basis of the current observational determinations for EG 50, this WD seems to be even denser than an iron WD.

At present, it seems that the physics that determines the radius of a WD star is fairly well understood, thus the indication of an iron core should not be expected to be due to some error in the treatment of equation of state of a degenerate plasma. Accordingly, if observations are confirmed to be accurate enough, we should seriously consider some physical process capable to produce an iron core for such low mass objects.

Detailed tabulations of the results presented in this paper are available upon request from the authors at their e-mail address.

Acknowledgements. O.G.B. wishes to acknowledge to Jan-Erik Solheim and the LOC of the 11th European Workshop on White Dwarfs held at Tromso (Norway) for their generous support that allowed him to attend that meeting were he became aware of the observational results that motivated the present work. We also acknowledge to our referee for his remarks and comments which significantly improved the original version of this work.

References

Alberts F., Savonije G.J., van der Heuvel E.P.J., Pols O.R., 1996, Nat. 380, 676
Alexander D.R., Ferguson J.W., 1994, ApJ 437, 879
Althaus L.G., Benvenuto O.G., 1997, ApJ 477, 313
Althaus L.G., Benvenuto O.G., 1998, MNRAS 296, 206
Benvenuto O.G., Althaus L.G., 1996a, Phys. Rev. D 53, 635
Benvenuto O.G., Althaus L.G., 1996b, ApJ 462, 364
Benvenuto O.G., Althaus L.G., 1997, MNRAS 288, 1004
Benvenuto O.G., Althaus L.G., 1998, MNRAS 293, 177

Benvenuto O.G., Althaus L.G., 1999, 11th European Workshop on White Dwarfs. Ed. J.E. Solheim, ASP Conference Series, in Press.
Burgers J.M., 1969, *Flow Equations for Composite Gases* (New York: Academic)
Callanan P. J., Garnavich P.M., Koester D., 1998, MNRAS 298, 207
Driebe T., Schönberner D., Blöcker T., Herwig F., 1998, A&A 339, 123
Edmonds P.D., Grindlay J., Cool A., et al. 1999, ApJ 516, 250
Ergma E., Sarna M. J., 1996, MNRAS 280, 1000
Glendenning N.K., Kettner Ch., Weber F., 1995a, Phys. Rev. Lett. 74, 3519
Glendenning N.K., Kettner Ch., Weber F., 1995b, ApJ 450, 253
Hamada T., Salpeter E.E., 1961, ApJ 134, 683
Hansen B. M. S., Phinney E. S. 1998, MNRAS 294, 557
Iben I. Jr., MacDonald J., 1985, ApJ 296, 540
Iben I. Jr., Tutukov A.V., 1984, ApJ 282, 615
Iben I. Jr., Tutukov A.V., 1986, ApJ 311, 742
Iglesias C.A., RogersF.J., 1993, ApJ 412, 752
Isern J., Canal R., Labay J., 1991, ApJ 372, L83
Itoh N., Kohyama Y., Matsumoto N., Seki M., 1984a, ApJ 285, 758
Itoh N., Kohyama Y., Matsumoto N., Seki M., 1984b, ApJ 285, 304
Itoh N., Kohyama Y., Matsumoto N., Seki M., 1987, ApJ 322, 584 (erratum)
Kippenhahn R., Weigert A., Hofmeister E., 1967, in Alder B, Fernbach S, Rottenberg M., eds. *Methods in computational Physics*, 7 (New York: Academic Press), 129
Koester D., 1978, A&A 64, 289
Koester D., Chanmugam G., 1990, Rep. Prog. Phys. 53, 837
Koester D., Schönberner D., 1986, A&A 154, 125
Landsman W., Aparicio J., Bergeron P., Di Stefano R., Stecher T.P., 1997, ApJ 481, L93
Marsh T. R., 1995, MNRAS 275, L1
Mazzitelli I., D'Antona F., 1986, ApJ 308, 706
Moran C., Marsh T.R., Bragaglia A., 1997, MNRAS 288, 538
Muchmore D., 1984, ApJ 278, 769
Paquette C., Pelletier C., Fontaine G., Michaud G., 1986, ApJS 61, 177
Provencal J.L., Shipman H.L., Hog E., Thejll P., 1998, ApJ 494, 759
Sarna M.J., Antipova J., Muslimov A., 1998, ApJ 499, 407
Saumon D., Chabrier G., Van Horn H.M., 1995, ApJS 99, 713
Savedoff M.P., Van Horn H.M., Vila S.C., 1969, ApJ 155, 221
Shapiro S.L., Teukolsky S.E., 1983, *Black Holes, White Dwarfs and Neutron Stars*, The Physics of Compact Objects, J. Wiley
van Kerkwijk M. H., Bergeron P., Kulkarni S. R., 1996, ApJ 467, L89
Vennes S., Fontaine G., Brassard P., 1995, A&A 296, 117
Wood M.A., 1995, In: Proc 9th European Workshop on White Dwarfs, eds. Koester D., Werner K. (Berlin: Springer), 41